

## Chapter 6

# The 5-fold *i*-Al-Pd-Mn Surface

In this chapter, a brief introduction to icosahedral quasicrystals including the indexing scheme of their diffraction patterns is presented first. The introduction is followed by the experimental details and characterization of the clean surface of *i*-Al<sub>71.5</sub>Pd<sub>21</sub>Mn<sub>8.5</sub> by He diffraction. Finally, surface phonons measured from the same surface are presented and discussed.

### Icosahedral Quasicrystals

Icosahedral quasicrystals are 3D quasicrystals possessing six 5-fold, ten 3-fold, and fifteen 2-fold rotational axes. A macroscopic view of an icosahedral quasicrystal displaying planes of different symmetries is shown in Figure 6.1. Like 1D and 2D quasicrystals, 3D quasicrystals can be described in terms of higher dimension periodic structures. Icosahedral quasicrystals can be obtained by an appropriate 3D cut of a 6D periodic lattice [5].

Among the many examples of icosahedral quasicrystals, Al-Pd-Mn is the most widely investigated because the structure of this phase has a very high degree of perfection and large grain samples have been available. From a point of view of surface researcher, *i*-Al-Pd-Mn, as other icosahedral quasicrystals, provides an opportunity to study a variety of high symmetry surfaces including the unique 5-fold surface.

### Indexing of the Diffraction Pattern

The reciprocal basis vectors of an icosahedral quasicrystal are shown in Figure 6.2. The six basis vectors point towards the corners of an icosahedra, and are defined by  $\mathbf{a}_1 = a(0, 0, 1)$

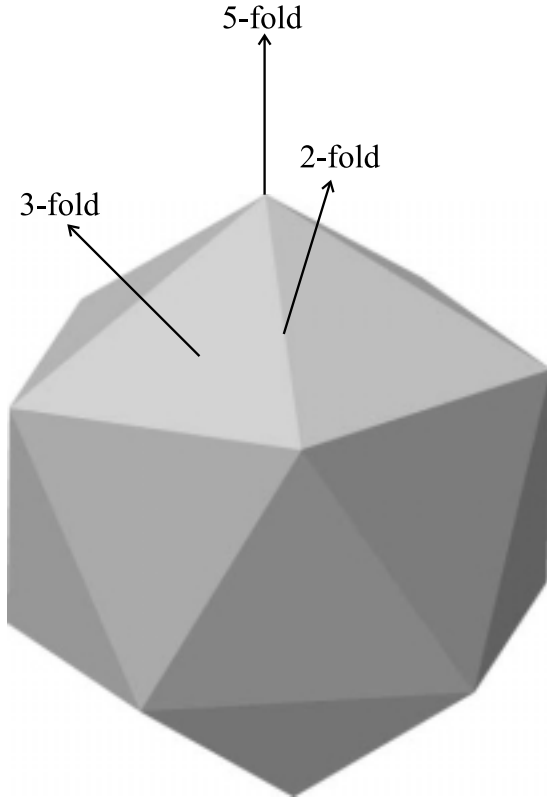


**Figure 6.1:** A macroscopic view of a 3D quasicrystal of icosahedral symmetry. It has six 5-fold, ten 3-fold, and fifteen 2-fold axes.

and  $\mathbf{a}_j = a(\sin \theta \cos \frac{2\pi j}{5}, \sin \theta \sin \frac{2\pi j}{5}, \cos \theta)$  for  $j = 2, \dots, 6$ , where  $\theta$  is the angle between two adjacent 5-fold axes ( $\tan \theta = 2$ ) and  $1/a$  is the lattice constant in 6D space [5]. These six basis vectors can be considered as the physical space projections of a 6D reciprocal basis given by

$$\mathbf{d}_1^* = a \begin{pmatrix} 0 \\ 0 \\ 1 \\ 0 \\ 0 \\ 1 \end{pmatrix}, \quad \mathbf{d}_j^* = a \begin{pmatrix} \sin \theta \cos \frac{2\pi j}{5} \\ \sin \theta \sin \frac{2\pi j}{5} \\ \cos \theta \\ -\sin \theta \cos \frac{4\pi j}{5} \\ -\sin \theta \sin \frac{4\pi j}{5} \\ -\cos \theta \end{pmatrix}, \quad j = 2, \dots, 6. \quad (6.1)$$

The diffraction vectors can be expressed by  $\mathbf{H}^{\parallel} = \sum_{j=1}^6 h_j \mathbf{a}_j$  with  $h_j$  integers. Each diffraction spot is characterized by six Miller indices  $(h_1 h_2 h_3 h_4 h_5 h_6)$ . The diffraction spots pointed to by  $\mathbf{a}_j$  ( $j = 1, \dots, 6$ ) are thus represented by  $(100000)$ ,  $(010000)$ ,  $(001000)$ ,  $(000100)$ ,  $(000010)$ , and  $(000001)$ , respectively, and the directions along the six 5-fold axes are  $[100000]$ ,  $[010000]$ ,  $[001000]$ ,  $[000100]$ ,  $[000010]$ , and  $[000001]$ .

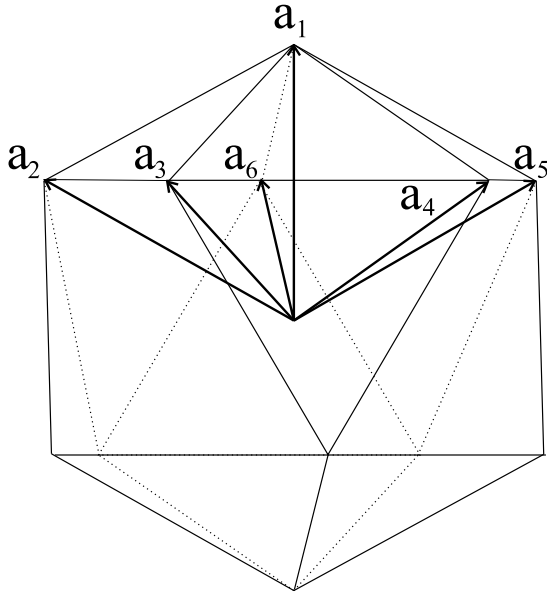


**Figure 6.2:** Illustration of the reciprocal basis vectors of an icosahedral quasicrystal. The six basis vectors  $\mathbf{a}_j$  ( $j = 1, \dots, 6$ ) are pointing from the center towards the corners of an icosahedra. The directions along the  $\mathbf{a}_j$  ( $j = 1, \dots, 6$ ) can be labeled by  $[100000]$ ,  $[010000]$ ,  $[001000]$ ,  $[000010]$ , and  $[000001]$ , respectively.

## 6.1 Characterization of the Clean Surface

A single grain  $\text{Al}_{71.5}\text{Pd}_{21}\text{Mn}_{8.5}$  quasicrystal was grown by the Czochralski method [152] and annealed for three months at  $820^\circ\text{C}$ . The sample was cut and mechanically polished perpendicular to the 5-fold axis prior to the surface treatments inside the UHV chamber. The single crystal surface was prepared by  $\text{Ne}^+$  ion bombardment (1-4 keV, for 30-60 minutes) and annealing at  $600^\circ\text{C}$  for 30-60 minutes. Experiments were performed in the UHV chamber (base pressure  $2 \times 10^{-10}$  mbar) discussed in Chapter 2.

A typical LEED pattern of the 5-fold  $i\text{-Al}_{71.5}\text{Pd}_{21}\text{Mn}_{8.5}(100000)$  surface is shown in Figure 6.3. The high symmetry directions of the surface can be represented by  $[001\bar{1}\bar{1}1]$  and  $[000\bar{1}10]$ . Helium diffraction along these high symmetry directions recorded at 22 meV beam energy are shown in Figure 6.4.

The ratio of specular intensity and higher order diffraction peaks in the observed spectra is on the order of ten suggesting a higher corrugation. Compared to the 10-fold and 2-fold surfaces of  $d\text{-Al-Ni-Co}$ , the surface has a moderate corrugation while the 10-fold surface has a much lower corrugation and the 2-fold surfaces have significantly higher corrugation. The result is consistent with the bulk terminated surfaces as the 10-fold surface consists of atoms lying in a single plane [66], while the possible termination of the 5-fold surface of  $i\text{-Al-Pd-Mn}$  [7] and 2-fold surfaces of  $d\text{-Al-Ni-Co}$  [66] are buckled surface layers [7].

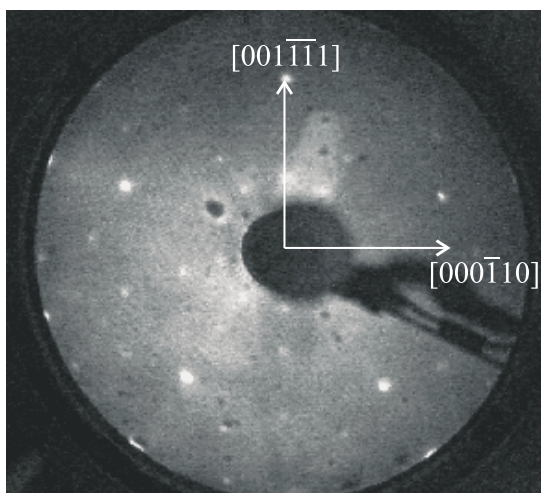


**Figure 6.3:** A typical LEED picture of 5-fold *i*-Al<sub>71.5</sub>Pd<sub>21</sub>Mn<sub>8.5</sub>(100000) surface at 63 eV electron energy. The high symmetry directions are represented by  $[001\bar{1}\bar{1}]$  and  $[000\bar{1}10]$ .

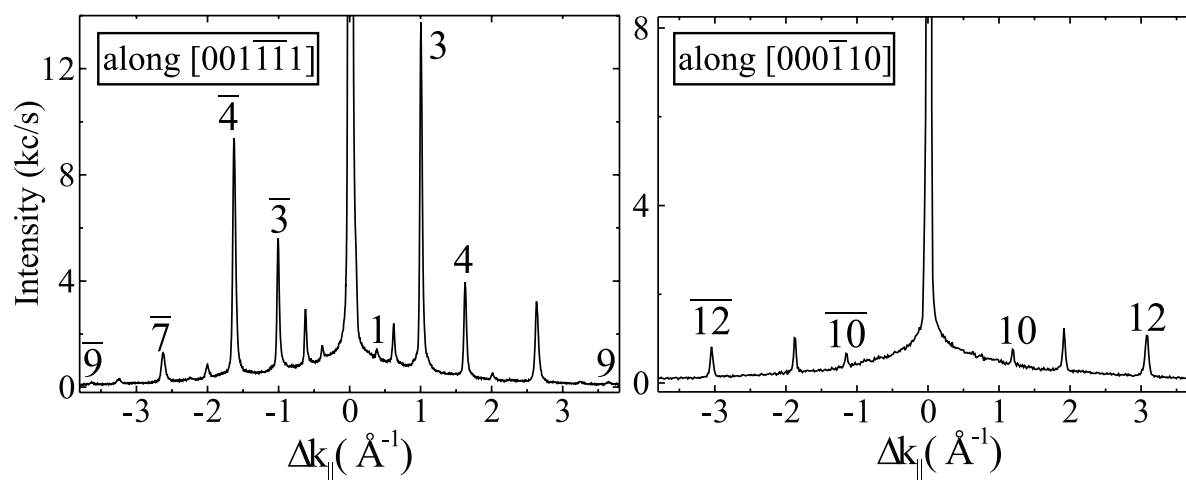


**Figure 6.4:** He diffraction along the  $[001\bar{1}\bar{1}]$  (left) and  $[000\bar{1}10]$  (right) directions at 22 meV beam energy.

The unique symmetry of the surface can be realized from the intensity distribution of diffraction peaks. As expected from the 5-fold LEED diffraction pattern, the intensity of peaks along  $[001\bar{1}\bar{1}]$  at wavevector  $k$  is different than that of their counterparts at  $-k$  (compare the intensity of peaks at  $\pm 0.99 \text{ \AA}^{-1}$ , marked by 3 and  $\bar{3}$  or at  $\pm 1.6 \text{ \AA}^{-1}$ , marked by 4 and  $\bar{4}$ ). The 5-fold symmetry is better illustrated in 2D diffraction pattern (Figure 6.5). The diffraction pattern is formed by using the position and intensity of peaks from the line scans shown in Figure 6.4. As the line scans along the two directions were measured from the surfaces under different conditions, the specular intensity of two directions is different. The displayed intensity in the 2D pattern is after normalization with respect to the background intensities.

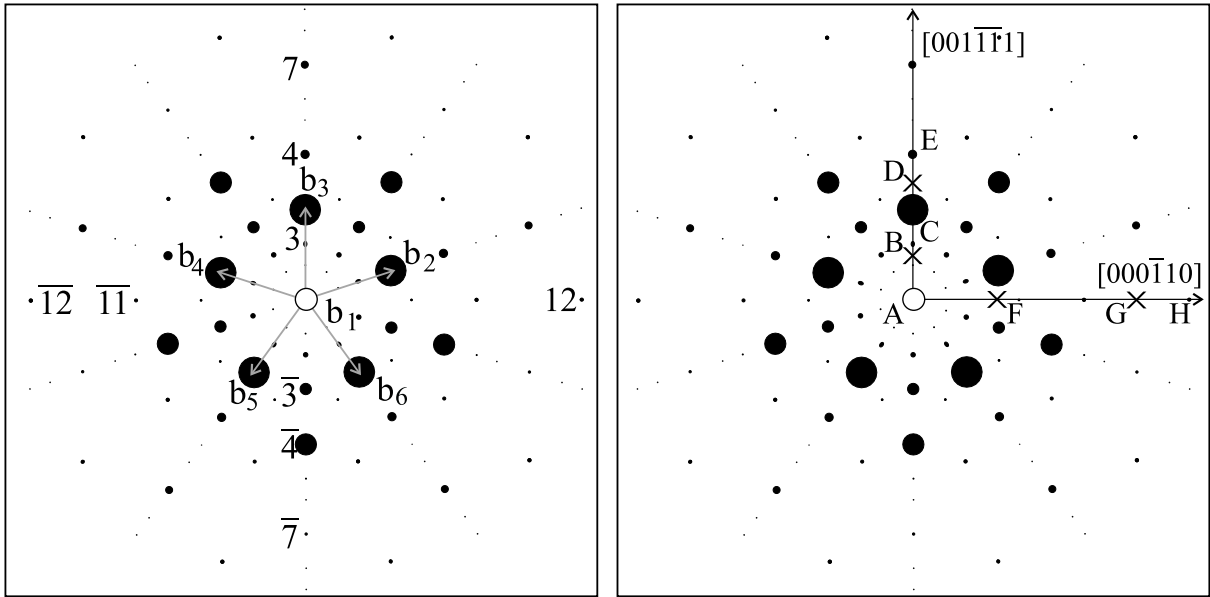


**Figure 6.5:** He diffraction of the 5-fold  $i\text{-Al}_{71.5}\text{Pd}_{21}\text{Mn}_{8.5}(100000)$  surface represented by solid circles. The radius of circles is proportional to the intensity (note the specular intensity is not scaled). The  $\mathbf{b}_j$  ( $j = 2, \dots, 6$ ) are the surface projected bulk reciprocal basis vectors (left). The high symmetry points of the QBZs are denoted by letters A, B, ... and the points marked by crosses are the QBZ boundaries (right).

The position of selected diffraction peaks are listed in Table 6.1 demonstrating the  $\tau$ -scaling relation. The diffraction vectors can be obtained by a linear combination of the surface projected bulk reciprocal basis vectors. The bulk basis  $\mathbf{a}_j$  ( $j = 1, \dots, 6$ ) can be decomposed into the components parallel and perpendicular to the surface as  $\mathbf{a}_j = (\mathbf{b}_j, b_{jz})$ . The surface projected components are shown by solid arrows in Figure 6.5, left, and defined by  $\mathbf{b}_1 = (0, 0)$  and  $\mathbf{b}_j$  ( $j = 2, \dots, 6$ ) =  $a(\sin \theta \cos \frac{2\pi j}{5}, \sin \theta \sin \frac{2\pi j}{5}) = b(\cos \frac{2\pi j}{5}, \sin \frac{2\pi j}{5})$  with  $b = a \sin \theta = 0.99 \text{ \AA}^{-1}$ .

## 6.2 Surface Phonons

Series of TOF spectra for different angles of incidence along the  $[001\bar{1}\bar{1}1]$  and  $[000\bar{1}10]$  directions recorded at a beam energy of 15 meV are shown in Figure 6.6, recorded at a sample temperature of around 200 °C.

As in the 10-fold surface of  $d\text{-Al-Ni-Co}$ , the TOF spectra consist of a central elastic peak, single phonon peaks, and background intensity. The single phonon peaks are sharp with the

Peaks	1	2	3	4	5	6
$\Delta k_{\parallel} / \text{\AA}^{-1}$	0.38	0.60	0.99	1.60	1.98	2.23
$\Delta k_{\parallel} / b$	$\tau^{-2}$	$\tau^{-1}$	1	$\tau$	2	$2\tau-1$
Peaks	7	8	9	10	11	12
$\Delta k_{\parallel} / \text{\AA}^{-1}$	2.60	3.19	3.6	1.15	1.88	3.06
$\Delta k_{\parallel} / b$	$\tau^2$	$2\tau$	$\tau^2+1$	$\chi$	$\chi\tau$	$\chi\tau^2$

**Table 6.1:** A list of diffraction vectors of the 5-fold *i*-Al<sub>71.5</sub>Pd<sub>21</sub>Mn<sub>8.5</sub>(100000) surface for selected peaks. The peak number follows Figure 6.4 or 6.5.

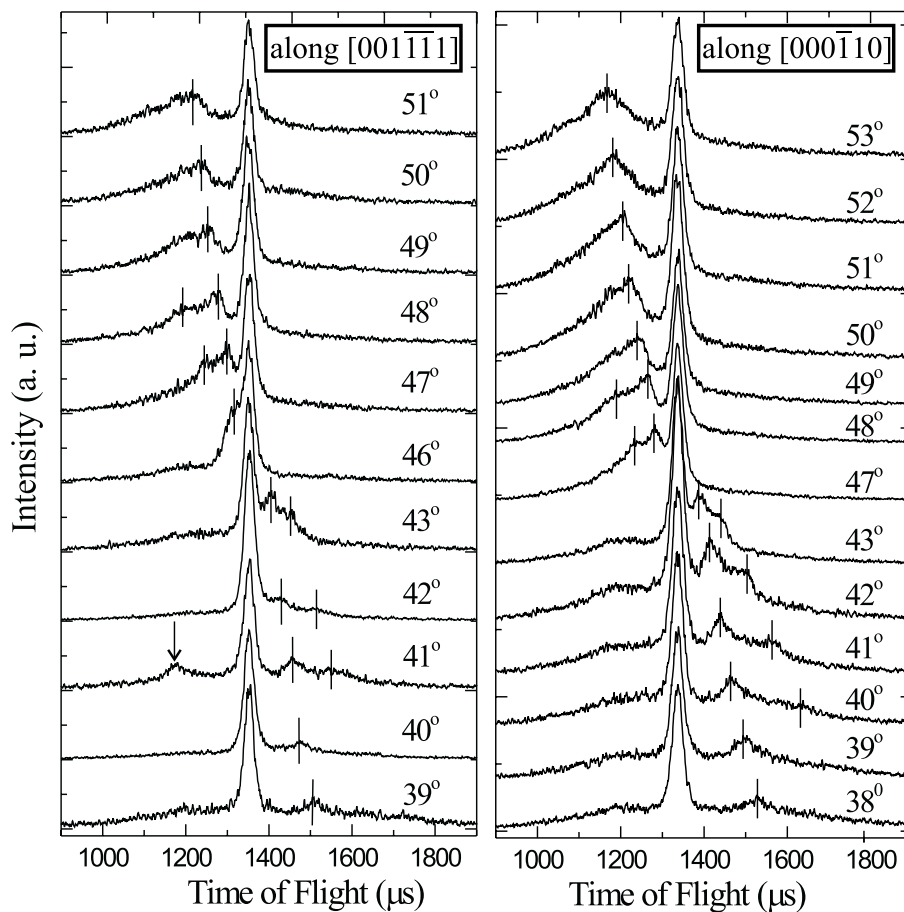


**Figure 6.6:** A series of TOF spectra along  $[001\bar{1}\bar{1}]$  (left) and  $[000\bar{1}10]$  (right) with a beam energy of 15 meV for different angles of incidence. Angles are given above spectra. Single phonon peaks are marked by vertical lines. The peak indicated by an arrow is a decepton.

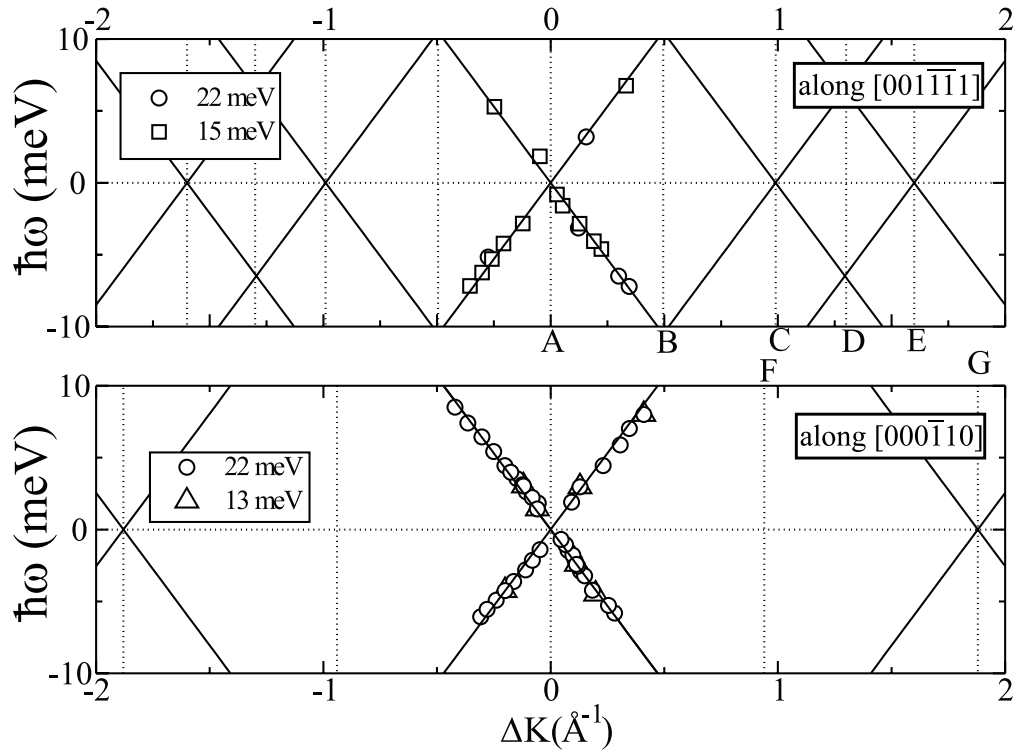


**Figure 6.7:** The phonon dispersion relation along the  $[001\bar{1}\bar{1}1]$  (upper) and  $[000\bar{1}10]$  (lower) azimuth. Different symbols represent the data obtained for different beam energy. The solid lines represent linear dispersion expected from the bulk ( $v_R = 3250$  m/s).

linewidth limited by the instrumental resolution for smaller wavevectors, while they are very broad for larger wavevectors, such that it is very hard to identify their position. The TOF spectrum at  $\theta_i = 41^\circ$  along  $[001\bar{1}\bar{1}1]$  is found to possess a decepton resulting from the diffraction peak at  $40.4^\circ$  ( $\Delta k_{\parallel} = -0.60 \text{ \AA}^{-1}$ ).

The dispersion relation derived from the TOF spectra are shown in Figure 6.7. The solid lines represent the linear dispersion, the slope of which is estimated from the Rayleigh mode velocity  $v_R$  expected from the bulk. The bulk velocities  $v_l = 6300 \pm 300$  m/s and  $v_t = 3500 \pm 100$  m/s [71] yields  $v_R = 3250 \pm 5\%$  m/s, which is slightly smaller than that of the  $d$ -Al-Ni-Co surface. All observed data in the dispersion relation fall on the linear regime. One can clearly see that the dispersion follows the linear relation expected from the bulk and that it is isotropic in this linear regime. The linearity holds up to a larger wavevector than in the 10-fold  $d$ -Al-Ni-Co surface. The bulk phonon dispersion (for transverse modes) of  $i$ -Al-Pd-Mn also holds a linear relation up to a larger wavevector than the dispersion of the  $d$ -Al-Ni-Co.

**Summary**

The 5-fold *i*-Al-Pd-Mn surface, similarly as the high symmetry surfaces of the *d*-Al-Ni-Co, shows a long range, bulk derived quasiperiodic order in the topmost surface layer. Helium diffraction reveals a moderate corrugation compared to the high symmetry surfaces of the *d*-Al-Ni-Co agreeing with the bulk terminated surfaces.

The surface possesses a well-defined Rayleigh mode. An isotropic sound velocity of about 3250 m/s is observed. The observed velocity agrees with the experimental bulk phonon data.

# Summary and Conclusion

Quasicrystals are a new class of material with long range order without periodicity, which often show conventionally forbidden rotational symmetries. Apart from the fascinating structure as well as the bulk-related physical properties, quasicrystals exhibit many interesting surface properties. Although many aspects of bulk structure of quasicrystals are well understood, many open questions regarding their surface structure remain.

The presented work focuses on surface studies of quasicrystals to get information about the fundamental features of the surfaces in this new class of material. The investigation is motivated by the following questions: Does the surface maintain a long range order? How is the surface structure related to the bulk? Are the surface features observed in periodic crystals plausible for quasicrystal surfaces? To investigate these, two different quasicrystals were chosen. Specifically, decagonal (*d*)  $\text{Al}_{71.8}\text{Ni}_{14.8}\text{Co}_{13.4}$  and icosahedral (*i*)  $\text{Al}_{71.5}\text{Pd}_{21}\text{Mn}_{8.5}$  were studied to determine their structure, morphology, and surface phonon dispersions.

These two quasicrystals are the most common systems used for surface studies due to the availability of large single grain samples. The decagonal quasicrystal belongs to the class of 2D quasicrystals with quasicrystalline planes stacked periodically along one direction, thus providing the possibility to study crystalline and quasicrystalline order in a single alloy. In contrast to 2D quasicrystals, the icosahedral quasicrystal has quasicrystalline order in all three dimensions. Moreover, the two systems provide an opportunity to study various types of high symmetry surfaces including the unusual 10-fold (in *d*-Al-Ni-Co) and 5-fold (in *i*-Al-Pd-Mn) surfaces.

The present works mainly focus on the surfaces of the *d*-Al-Ni-Co. All existing low index surfaces, namely the 10-fold (00001), the 2-fold (10000), and the 2-fold (001 $\bar{1}$ 0) were studied. The [10000] and [001 $\bar{1}$ 0] directions represent the two inequivalent sets of 2-fold axes appearing alternately at 18° in the plane perpendicular to the [00001] (10-fold) axis. Both 2-fold (10000)

and  $(001\bar{1}0)$  surfaces thus have a common high symmetry direction along the 10-fold axis. The investigation of all high symmetry surfaces provides an opportunity to learn about the relative stability of different surfaces.

Different experimental techniques capable of providing information both in real and reciprocal space were used. To relate the structure of the topmost layer with that of the surface region (up to several topmost layers), highly surface sensitive elastic He atom scattering (HAS) and high resolution spot profile analyzing low energy electron diffraction (SPA-LEED) were employed. In addition to providing information of average structure and limited morphological insights of the topmost layer, HAS is appropriate to characterize the surface quality due to its extremely high sensitivity to all types of defects such as vacancies, adatoms, and steps. To determine other features which cannot be achieved by diffraction techniques such as details on step morphology, local defects, and tiling, the 10-fold surface was imaged by low temperature (6 K) scanning tunneling microscopy (LT-STM) in real space at near atomic resolution. Surface phonons were investigated by inelastic He atom scattering, which is a unique technique to study low energy phonons (the Rayleigh mode).

Surfaces prepared by sputtering and annealing are found to possess a high structural quality suitable for He diffraction. However, the surface termination is found to be dependent on preparation conditions (particularly the 10-fold  $d$ -Al-Ni-Co surface). The surface prepared at lower annealing temperature shows less intense peaks in He diffraction and its STM images reveal two types of surface terminations (fine and coarse structure) in a single terrace, very rough steps, and narrow terraces. All of these demonstrate that the surface does not reach to its equilibrium at low annealing temperatures. Annealing to higher temperature always yields a more ordered structure.

The topmost layer of all surfaces maintains the rotational symmetry of their respective bulk. Observed diffraction spots are very sharp with widths limited by the instrumental resolution giving evidence of perfect long range order in the topmost surface layer. The correlation length is as good as that normally observed in periodic crystal surfaces, where a long range order is established due to the lattice periodicity.

The diffraction patterns are consistent with those of bulk terminated surfaces. In addition to the peak positions matching the projections of the respective bulk reciprocal lattice structure, He diffraction shows a surface corrugation expected for the bulk terminated surfaces. Other

bulk features like the periodicity and the superstructure are also apparent in the diffraction of the *d*-Al-Ni-Co surfaces. Aside from these known bulk features, the 2-fold surfaces exhibit a new periodicity of 16 Å. Both HAS and SPA-LEED show equally weak peaks corresponding to the 16 Å periodicity, demonstrating that it is a bulk feature.

As expected in the bulk derived structure, the diffraction vectors are related by the golden mean ( $\tau = 1.618\dots$ , an irrational number related to the pentagonal and decagonal symmetry). The diffraction spots are densely distributed in the reciprocal space. The dense spots can be derived by an irrational projection of higher dimension reciprocal lattice structure into the physical space. Furthermore, the diffraction pattern exhibits a hierarchy of spots (particularly the 2-fold *d*-Al-Ni-Co(10000) surface), which can be explained on the basis of a Fibonacci lattice, a well-known prototype of 1D quasiperiodic structures.

As normally seen in periodic crystal surfaces, step-terrace formation is observed in the 10-fold *d*-Al-Ni-Co surface. STM images of the surface show atomically flat terraces with a corrugation of a few tenths of an Angstrom. The terraces are separated by steps of monoatomic height. The terraces exhibit different types of 5-fold symmetric features correlated by a long range quasicrystalline order. In spite of a careful surface preparation and the application of a high performance microscope, atomic resolution of the surface could not be achieved. The best resolution obtained was  $\sim 3$  Å. Even with this resolution, the STM image can be overlaid by a rhombic tiling. The vertices of the tiling are located at the centers of 20 Å diameter clusters. Determining the tiling is far from trivial. With an intensive search, only one image is found to demonstrate the tiling on a large area of a terrace.

In addition to the above described structure and step terrace morphology of the surface, a surface energy related phenomena observed in periodic crystals, the faceting, was also observed in quasicrystals. The faceting is caused by the tendency of a crystal to lower its surface free energy. The 2-fold (001 $\bar{1}$ 0) surface was found to develop facets of (10000)-equivalent orientation due to a lower surface energy of the (10000)- compared to the original (001 $\bar{1}$ 0)-surface.

With the successful preparation of surfaces with high structural quality, it became possible to measure surface phonons on the 10-fold surface of the *d*-Al-Ni-Co and the 5-fold surface of the *i*-Al-Pd-Mn. Both surfaces show a well defined Rayleigh mode with isotropic sound velocities agreeing with the respective bulk phonons measurements data. As expected for an acoustic phonon branch, the dispersion relation holds a linear *k*-dependent up to a certain wavevector

and starts to bend down with increasing  $k$ -value. From the observed dispersion relation, the quasi-Brillouin zone (QBZ) centers are identified at the strong Bragg peaks and QBZ boundaries at half way between the two consecutive strong Bragg peaks.

To conclude, despite their very complex atomic structure and lacking periodicity, quasicrystals yield high quality surfaces under suitable preparation that exhibit a very rich variety of structural and morphological properties. The quality of surfaces is comparative to that of periodic crystal surfaces. A long range correlation is maintained even on the topmost surface layer. Phenomenon observed in periodic crystals surfaces such as step-terrace formation, faceting, bulk termination, and surface phonons are also found in quasicrystals surfaces. However, other surface features like reconstruction have yet to be observed. Structure and dynamics of the surface very closely reflect the underlying bulk properties. Finally, a better understanding of the clean surfaces has opened a way to investigate a possible relationship of the unique structure to the outstanding surface properties.